entropy

MDPI

*Review*

# Economics and Finance: *q*-Statistical Stylized Features Galore

**Constantino Tsallis** [1,2,3]

[1] Centro Brasileiro de Pesquisas Físicas and National Institute of Science and Technology for Complex Systems, Rua Xavier Sigaud 150, Urca, Rio de Janeiro 22290-180, Brazil; tsallis@cbpf.br; Tel.: +55-(21)-2141-7190
[2] Santa Fe Institute, 1399 Hyde Park Road, Santa Fe, NM 87501, USA
[3] Complexity Science Hub Vienna, Josefstädter Strasse 39, Vienna 1080, Austria

Received: 4 August 2017; Accepted: 29 August 2017; Published: 31 August 2017

**Abstract:** The Boltzmann–Gibbs (BG) entropy and its associated statistical mechanics were generalized, three decades ago, on the basis of the nonadditive entropy $S_q$ ($q \in \mathcal{R}$), which recovers the BG entropy in the $q \to 1$ limit. The optimization of $S_q$ under appropriate simple constraints straightforwardly yields the so-called $q$-exponential and $q$-Gaussian distributions, respectively generalizing the exponential and Gaussian ones, recovered for $q = 1$. These generalized functions ubiquitously emerge in complex systems, especially as economic and financial stylized features. These include price returns and volumes distributions, inter-occurrence times, characterization of wealth distributions and associated inequalities, among others. Here, we briefly review the basic concepts of this $q$-statistical generalization and focus on its rapidly growing applications in economics and finance.

**Keywords:** economics and finance; nonadditive entropies; nonextensive statistical mechanics

## 1. Introduction

Exponential and Gaussian functions ubiquitously emerge within linear theories in mathematics, physics, economics and elsewhere. To illustrate in what sense they are linear, let us focus on three typical mathematical situations, namely an ordinary differential equation, a partial derivative equation and an entropic optimization.

Consider the following ordinary differential equation:

$$\frac{dy}{dx} = ay \quad [y(0) = 1]\,. \tag{1}$$

The solution is the well-known exponential function:

$$y = e^{ax}\,. \tag{2}$$

Consider now the following partial derivative equation:

$$\frac{\partial p(x,t)}{\partial t} = D\frac{\partial^2 p(x,t)}{\partial x^2} \quad [D > 0;\, t \geq 0;\, p(x,0) = \delta(x)]\,, \tag{3}$$

where $\delta(x)$ is the Dirac delta function. The solution is the well-known Gaussian distribution:

$$p(x,t) = \frac{1}{\sqrt{2\pi Dt}} e^{-x^2/2Dt}\,. \tag{4}$$

Let us finally consider the following entropic functional:

$$S_{BG} = -k \int dx\, p(x) \ln p(x) \quad (k > 0) \tag{5}$$

with the constraint:

$$\int dx\, p(x) = 1\,, \tag{6}$$

where BG stands for Boltzmann–Gibbs; $k$ is a conventional positive constant (usually $k = k_B$ in physics, and $k = 1$ elsewhere). If we optimize the functional (5) with the constraint (6) and:

$$\langle \epsilon(x) \rangle \equiv \int dx\, p(x)\epsilon(x) = u \quad (u \in \mathcal{R}) \tag{7}$$

$\epsilon(x)$ being bounded below, we obtain:

$$p(x) = \frac{e^{-\beta\epsilon(x)}}{\int dx\, e^{-\beta\epsilon(x)}}\,, \tag{8}$$

where $\beta \equiv 1/kT$ is the Lagrange parameter associated with Constraint (7); $T$ is the absolute temperature within BG statistical mechanics (necessarily $T > 0$ if $\epsilon(x)$ is unbounded from above; but both $T > 0$ and $T < 0$ possibilities exist if $\epsilon(x)$ is bounded also from above). The probability distribution $p(x)$ corresponds to the celebrated BG weight, where $Z \equiv \int dx\, e^{-\beta\epsilon(x)}$ is usually referred to as the partition function. Two particular cases emerge frequently. The first of them is $\epsilon(x) = x \;\; (x \geq 0)$ with $u \equiv \langle x \rangle$, hence $p(x) = \frac{e^{-x/\langle x \rangle}}{\langle x \rangle}$, thus recovering solution (2). The second one is $\epsilon(x) = x^2$ with $u \equiv \langle x^2 \rangle$, hence $p(x) = \frac{e^{-x^2/2\langle x^2 \rangle}}{\sqrt{2\pi\langle x^2 \rangle}}$, thus recovering solution (4). Therefore, basic cases connect $S_{BG}$ with the solutions of the linear Equations (1) and (3). In addition to that, let us make explicit in what sense $S_{BG}$ is itself linear. We consider a system $(A+B)$ constituted by two probabilistically independent subsystems $A$ and $B$. In other words, we consider the case where the joint probability of $(A+B)$ factorizes, i.e., $p^{(A+B)}(x,y) = p^{(A)}(x)p^{(B)}(y)$ $[\forall (x,y)]$. We straightforwardly verify that the functional $S_{BG}$ is additive in the sense of Penrose [1], namely that:

$$S_{BG}(A+B) = S_{BG}(A) + S_{BG}(B)\,. \tag{9}$$

In the present brief review, we shall address a special class of nonlinearities, namely those emerging within nonextensive statistical mechanics, $q$-statistics for short [2–6].

Equation (1) is now generalized into the following nonlinear one:

$$\frac{dy}{dx} = ay^q \quad [y(0) = 1;\, q \in \mathcal{R}]\,. \tag{10}$$

Its solution is:

$$y = e_q^{ax}\,, \tag{11}$$

where the $q$-exponential function is defined as $e_q^z \equiv [1 + (1-q)z]_+^{1/(1-q)}$ $(e_1^z = e^z)$, with $[1 + (1-q)z]_+ = 1 + (1-q)z$ if $z > 0$ and zero otherwise. Its inverse function is the $q$-logarithm, defined as $\ln_q z \equiv \frac{z^{1-q}-1}{1-q}$ $(\ln_1 z = \ln z)$. To avoid any confusion, let us mention that many other $q$-deformations of the exponential and logarithmic functions have been introduced in the literature for a variety of purposes; among them, we have for instance Ramanujan's $q$-exponential function, unrelated to the present one.

Equation (3) is now generalized into the following nonlinear one (referred to in the literature as the porous medium equation [7–9]):

$$\frac{\partial p(x,t)}{\partial t} = D_q \frac{\partial^2 [p(x,t)]^{2-q}}{\partial x^2} \quad [D_q(2-q) > 0;\, D_1 \equiv D;\, q < 3;\, t \geq 0;\, p(x,0) = \delta(x)]\,. \tag{12}$$

Its solution generalizes Equation (4) and is given by:

$$p(x,t) = \frac{1}{\sqrt{\pi A_q}} e_q^{-x^2/\{A_q[(D_q)t]^{\frac{2}{3-q}}\}} \tag{13}$$

with:

$$A_q = \begin{cases} \dfrac{\sqrt{q-1}\,\Gamma\left(\frac{1}{q-1}\right)}{\Gamma\left(\frac{3-q}{2(q-1)}\right)} & \text{if } 1 < q < 3\,, \\ 2 & \text{if } q = 1\,, \\ \dfrac{\sqrt{1-q}\,\Gamma\left(\frac{5-3q}{2(1-q)}\right)}{\Gamma\left(\frac{2-q}{1-q}\right)} & \text{if } q < 1\,. \end{cases} \tag{14}$$

Before going on, let us mention that solution (13) implies that $x^2$ scales like $t^{\frac{2}{3-q}}$, hence normal diffusion for $q = 1$, anomalous sub-diffusion for $q < 1$ and super-diffusion for $1 < q < 3$, which has recently been impressively validated (within a 2% experimental error) in a granular medium [10]. The important connection between the power-law nonlinear diffusion (12) and the entropy $S_q$ described here below was first established by Plastino and Plastino in [11], where they considered a more general evolution equation that reduces to (12) in the particular case of vanishing drift (i.e., $F(x) = 0$, $\forall x$). The Plastino–Plastino Equation [11] $\frac{\partial p(x,t)}{\partial t} = -\frac{\partial}{\partial x}[F(x)p(x,t)] + D_q \frac{\partial^2 [p(x,t)]^{2-q}}{\partial x^2}$ with $F(x) = -dV(x)/dx$ generalizes the porous medium equation in the same sense that the linear Fokker–Planck equation generalizes the classical heat equation. The above nonlinear Equations (10) and (12) have been addressed here in order to provide some basic mathematical structure to approaches of various economic- and financial-specific features presented later on.

Let us now focus on the entropic functional $S_q$ upon which nonextensive statistical mechanics is based. It is defined as follows:

$$S_q \equiv k\frac{1-\int dx\,[p(x)]^q}{q-1} = k\int dx\, p(x) \ln_q \frac{1}{p(x)} = -k\int dx\,[p(x)]^q \ln_q p(x) = -k\int dx\, p(x) \ln_{2-q} p(x) \tag{15}$$

with $S_1 = S_{BG}$. If we optimize this functional with the constraints (6) and:

$$\langle \epsilon(x) \rangle_q \equiv \frac{\int dx\,[p(x)]^q \epsilon(x)}{\int dx\,[p(x)]^q} = u_q \quad (u_q \in \mathcal{R};\, u_1 = u) \tag{16}$$

we obtain [4]:

$$p(x) = \frac{e_q^{-\beta_q \epsilon(x)}}{\int dx\, e_q^{-\beta_q \epsilon(x)}} = \frac{e_q^{-\beta_q'[\epsilon(x)-u_q]}}{\int dx\, e_q^{-\beta_q'[\epsilon(x)-u_q]}} \quad (\beta_1 = \beta_1' = \beta)\,. \tag{17}$$

As before, two particular cases emerge frequently. The first of them is $\epsilon(x) = x \ \ (x \geq 0)$ with $u_q \equiv \langle x \rangle_q$; hence, $p(x)$ recovers the form of (11). The second one is $\epsilon(x) = x^2$ with $u_q \equiv \langle x^2 \rangle_q$; hence, $p(x)$ recovers the form of solution (13). Finally, if we consider $S_q$ itself for two independent subsystems $A$ and $B$, we straightforwardly verify the following nonlinear composition law:

$$\frac{S_q(A+B)}{k} = \frac{S_q(A)}{k} + \frac{S_q(B)}{k} + (1-q)\frac{S_q(A)}{k}\frac{S_q(B)}{k}\,, \tag{18}$$

hence

$$S_q(A+B) = S_q(A) + S_q(B) + \frac{1-q}{k} S_q(A) S_q(B)\,. \tag{19}$$

We then say that $S_q$ is nonadditive for $q \neq 1$. Entropic additivity is recovered if $(1-q)/k \to 0$, which can occur in two different circumstances: $q \to 1$ for fixed $k$ or $k \to \infty$ for fixed $q$. Since $k$ always appears in physics in the form $kT$, the limit $k \to \infty$ is equivalent to $T \to \infty$. This is, by the way, the basic reason for which, in the limit of high temperatures or low energies, Maxwell–Boltzmann statistics, Fermi–Dirac, Bose–Einstein and $q$-statistics asymptotically coincide.

The above $q$-generalized thermostatistical theory has been useful in the study of a considerable number of natural, artificial and social systems (see [12]). Theoretical and experimental illustrations in natural systems include long-range-interacting many-body classical Hamiltonian systems [13–20] (see also [21,22]; the study of the long-range version of [23] would surely be interesting), dissipative many-body systems [24], low-dimensional dissipative and conservative nonlinear dynamical systems [25–31], cold atoms [32–34], plasmas [35,36], trapped atoms [37], spin-glasses[38], power-law anomalous diffusion [39,40], granular matter [10], high-energy particle collisions [41–46], black holes and cosmology [47,48], chemistry [49], earthquakes [50], biology [51,52], solar wind [53,54], anomalous diffusion in relation to central limit theorems and overdamped systems [55–64], quantum entangled systems [65,66], quantum chaos [67], astronomical systems [68,69], thermal conductance [70], mathematical structures [71–76] and nonlinear quantum mechanics [77–96], among others. Illustrations in artificial systems include signal and image processing [97,98] and (asymptotically) scale-free networks [99–101]. In the realm of social systems, from now on, we focus on economics and financial theory [102–118].

## 2. Applications in Economics and Finance

### 2.1. Prices and Volumes

Time series of prices $p_t$ (say of stocks, commodities, etc.), where $t$ runs along chosen units (say seconds or minutes, or days, or years) are conveniently replaced by their corresponding returns (or logarithmic returns), defined as follows:

$$r_t = \ln \frac{p_{t+1}}{p_t} \simeq \frac{p_{t+1} - p_t}{p_t} \quad (t = 0, 1, 2, \dots)\,. \tag{20}$$

Returns do not depend on the specific currency of the prices and fluctuate around zero; in addition to that, their definition cancels systematic inflation. The distribution of returns usefully characterizes the price fluctuations. See an illustration in Figure 1, from [103] (see also [104,118]). The amounts of the corresponding transactions are currently referred to as volumes: see, for example, Figure 2.

### 2.2. Volatilities

The volatility characterizes the size (standard deviation) of the fluctuations of returns. The volatility smile characterizes the correction of empirical volatilities with regard to a Gaussian-based expectation: see an illustration in Figure 3 (from [103]). To be more explicit, let us assume that we are handling the following Gaussian distribution $\propto e^{-\mathcal{B}r^2}$, where $\mathcal{B}$ characterizes univocally the volatility. To discuss the probability distribution of quantities such as $\mathcal{B}$, Queiros introduced [108] the $q$-log normal probability function:

$$p_q(x) = \frac{1}{Z_q x^q} e^{-\frac{[\ln_q x - \mu]^2}{2\sigma^2}} \quad (x > 0)\,, \tag{21}$$

where $Z_q$ is a normalizing factor and $(q, \mu, \sigma)$ are parameters. The $q = 1$ particular case corresponds to the standard log-normal function. See Figure 4 for illustrative examples of this function. See also Figure 5 for a real financial application.

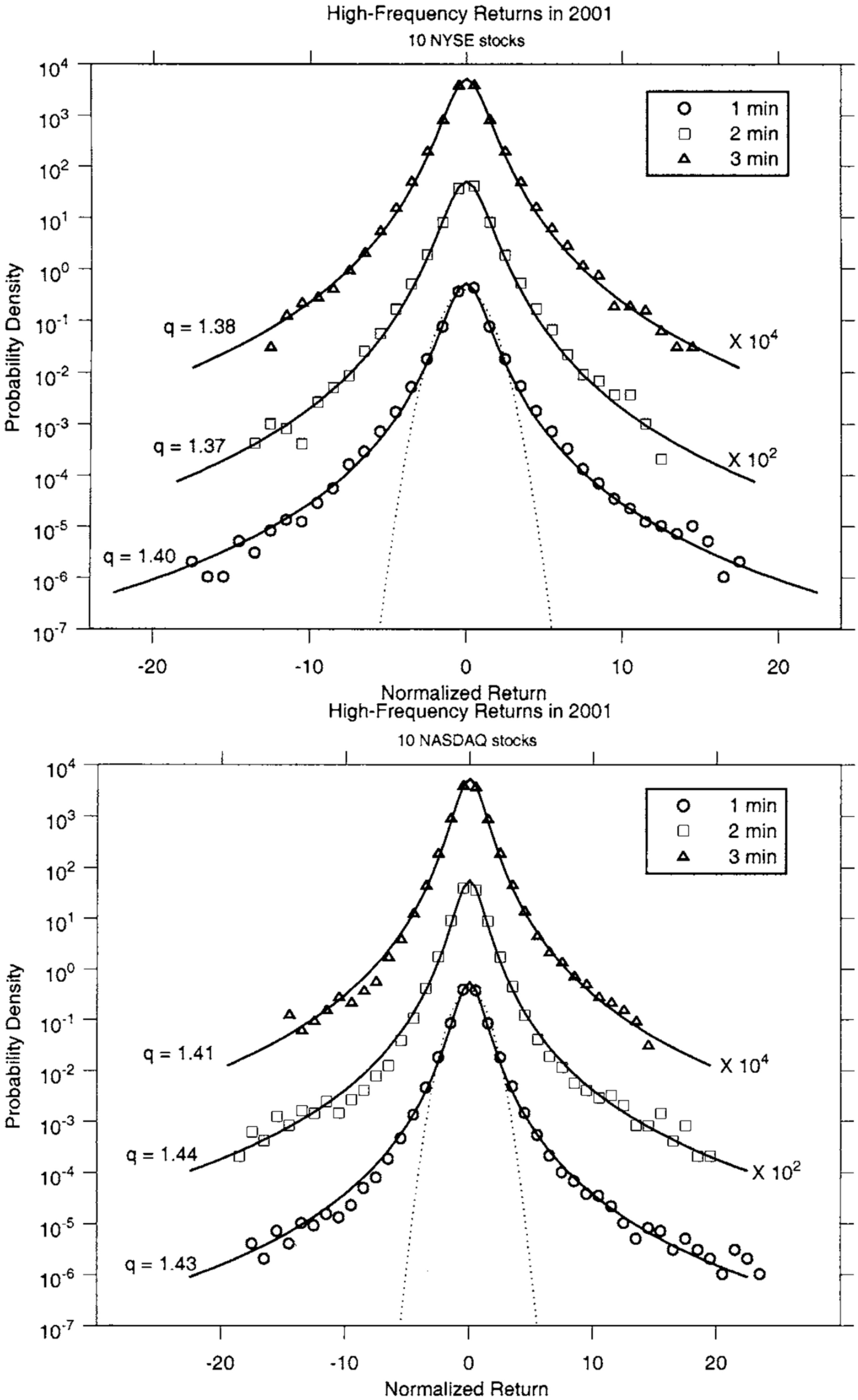


**Figure 1.** Empirical return densities (points) and $q$-Gaussians (solid lines) for normalized returns of the 10 top-volume stocks in the NYSE and in NASDAQ in 2001. The dotted line is a (visibly inadequate) Gaussian distribution. The 2- and 3-min curves are moved vertically for display purposes. From [103]. There exist in the literature quite a few other such examples, for other stocks and other years, with similar values of $q$.

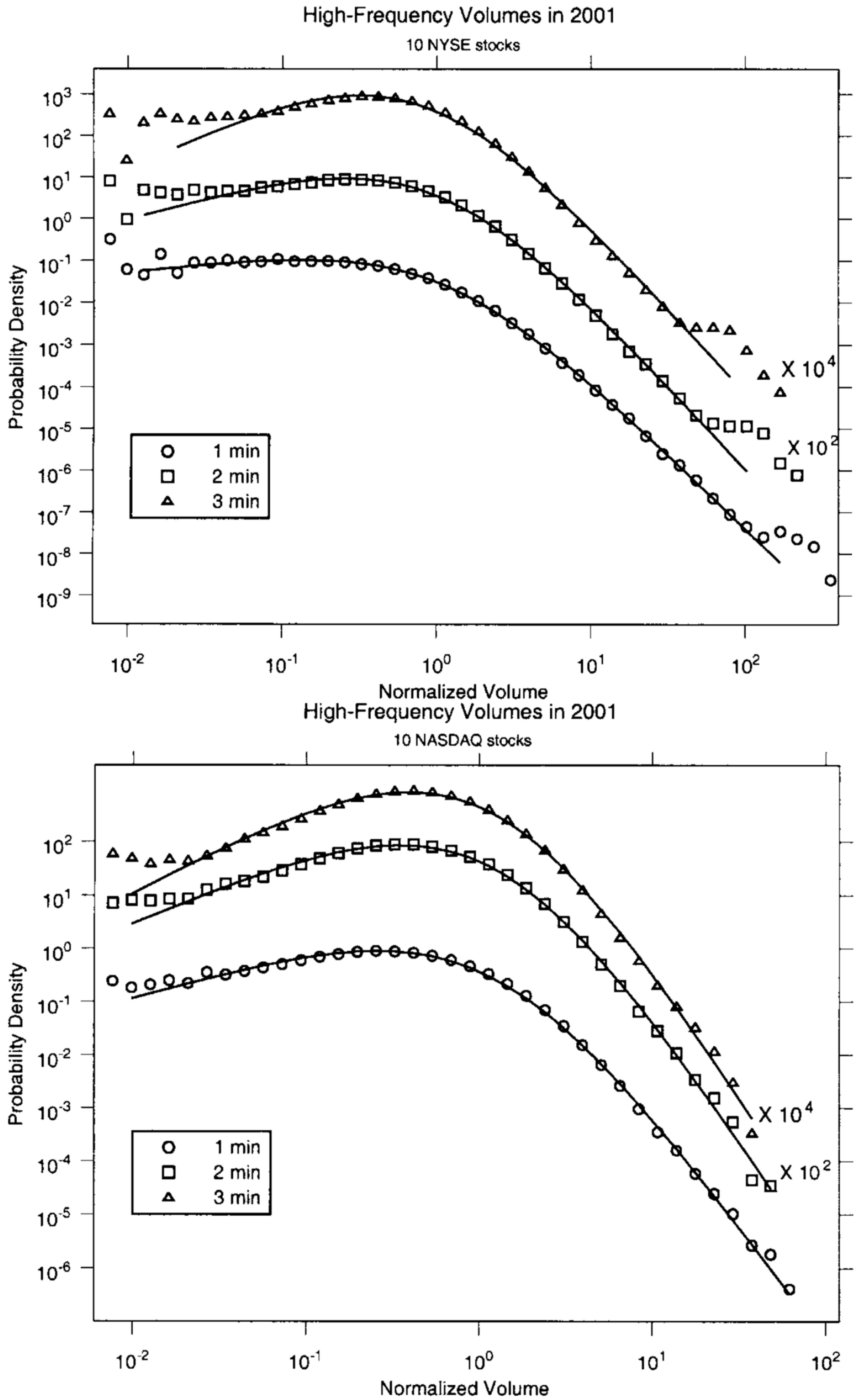


**Figure 2.** Empirical distributions (points) and $q$-exponential-like curves (solid lines) for normalized volumes of the 10 top-volume stocks in the NYSE and in the NASDAQ in 2001. The solid lines are fittings with a $q$-exponential multiplied by a power-law (analogous to the density of states prefactor that typically emerges for the distributions of quasi-particles in, say, condensed matter physics); from [103]. There exist in the literature quite a few other such examples, for other stocks and other years, with similar values of $q$ and of the rest of the fitting indices.

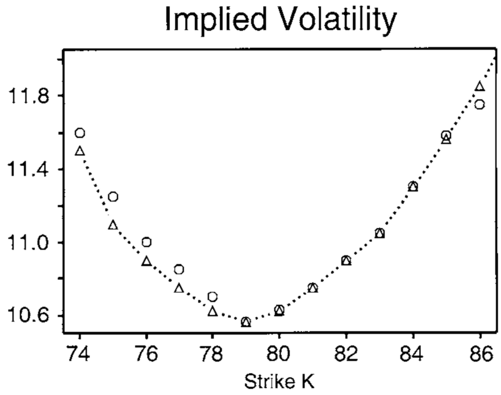


**Figure 3.** Implied volatilities as a function of the strike price for call options on JY currency futures, traded on 16 May 2002, with 147 days left to expiration. In this typical example, the current price of a contract on Japanese futures is \$79, and the risk-free rate of return is 5.5%. Circles correspond to volatilities implied by the market, whereas triangles correspond to volatilities implied by our model with $q = 1.4$ and $\sigma = 10.2\%$. The dotted line is a guide to the eye. From [103].

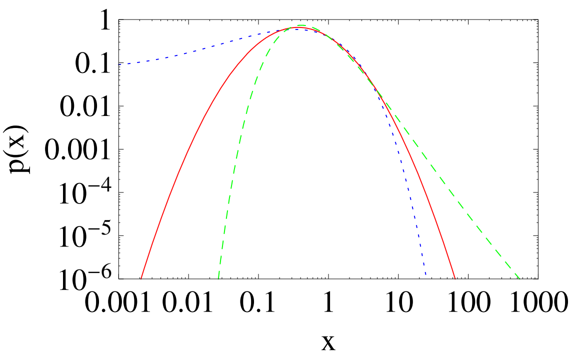


**Figure 4.** Illustrations of the $q$-log-normal density for $\mu = 0$ and $\sigma = 1$: blue $q = 5/4$, red $q = 1$ and green $q = 4/5$. From [108].

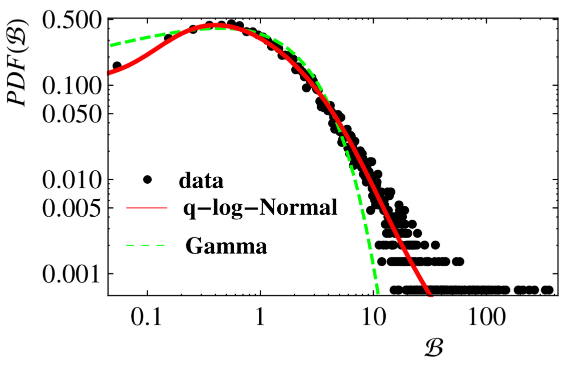


**Figure 5.** Probability density function of a five-day volatility vs. $\mathcal{B}$. The symbols are obtained from the data, and the lines are the best fits with the Gamma distribution (dashed green) and the double-sided $q$-log-normal (red) with $\mu = 0.391$, $\sigma = 1.15$ and $q = 1.22$. For further details, see [108].

### 2.3. Inter-Occurrence Times

We can see in Figure 6 two typical time series of price returns, together with a chosen threshold $Q = -0.037$, which corresponds to an average inter-occurrence time $R_Q = 70$ [106,107]. The quantity $R_Q$ monotonically increases with $|-Q|$ in each one of the examples shown in Figures 7 and 8. For a fixed value of $R_Q$, we verify that $p_Q(r) \propto e_{q_{threshold}}^{-\beta_{threshold}\, r}$, with:

$$q_{threshold} = 1 + q_0 \ln(R_Q/2) \quad (q_0 \simeq 0.168)\,. \tag{22}$$

See the illustrations in Figures 9 and 10. The fact that we have analytically $p_Q(r)$ enables us to straightforwardly obtain an explicit expression for the risk function $W_Q(t;\Delta t)$, which is defined as the probability of having once again a fluctuation larger than $|-Q|$ within an interval $\Delta t$ at time $t$ after the last large fluctuation. It can be shown [106,109] that:

$$W_Q(t;\Delta t) \equiv \frac{\int_t^{t+\Delta t} p_Q(r)dr}{\int_t^{\infty} p_Q(r)dr} = 1 - \left[1 + \frac{\beta_{threshold}(q_{threshold}-1)\Delta t}{1+\beta_{threshold}(q_{threshold}-1)t}\right]^{\frac{q_{threshold}-2}{q_{threshold}-1}} = 1 - \frac{e_{\tilde{q}}^{-(\beta_{threshold}/\tilde{q})(t+\Delta t)}}{e_{\tilde{q}}^{-(\beta_{threshold}/\tilde{q})t}} \tag{23}$$

with $\tilde{q} \equiv 1/(2 - q_{threshold})$. See Figure 11.

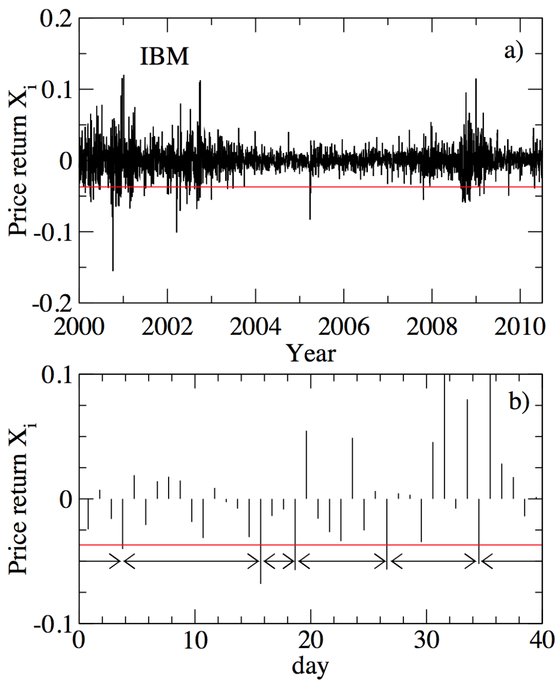


**Figure 6.** Illustration of the relative daily price returns $X_i$ of the IBM stock between (**a**) January 2000 and June 2010 and (**b**) 27 August and 23 October 2002. The red line shows the threshold $Q \simeq -0.037$, which corresponds to an average inter-occurrence time of $R_Q = 70$. In (b), the inter-occurrence times are indicated by arrows. From [106].

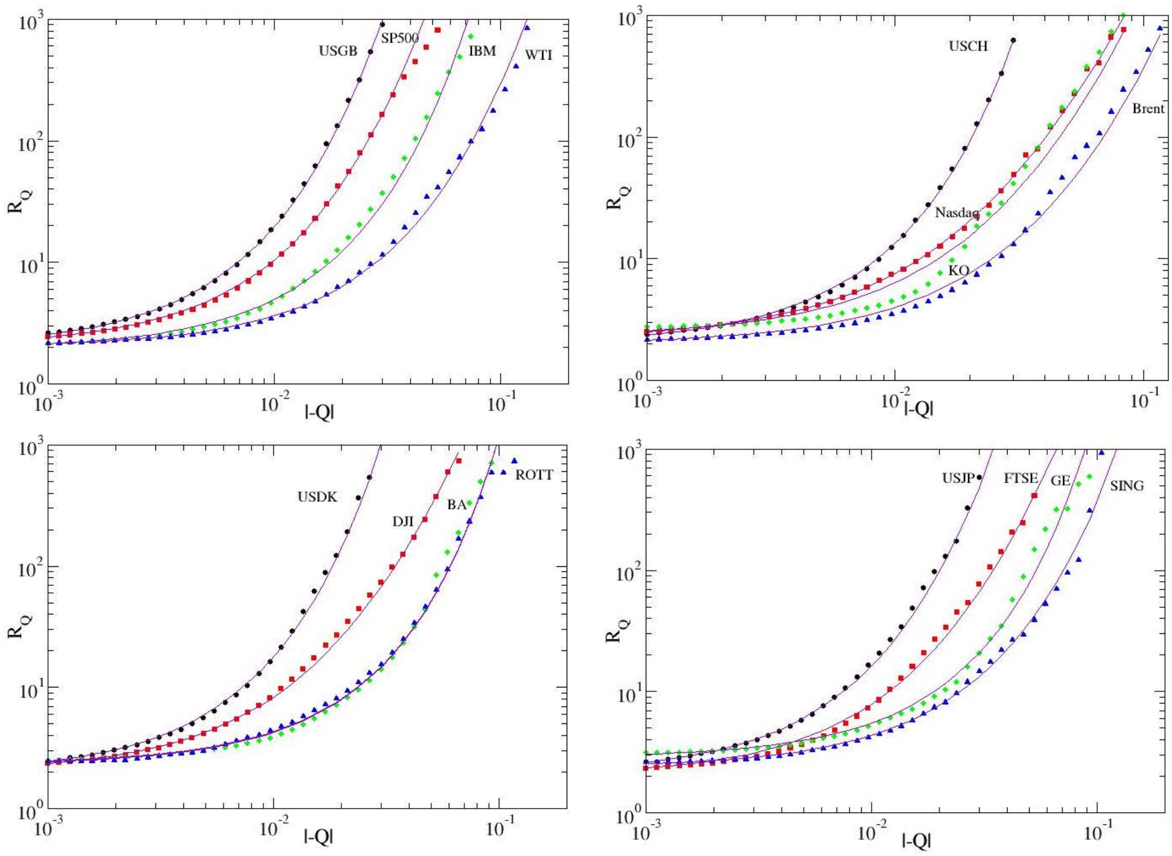


**Figure 7.** The mean inter-occurrence time $R_Q$ vs. the absolute value of the loss threshold $-Q$. The continuous curves are fittings with $R_Q = Ae_{q_{inter}}^{B_{inter}|Q|} = A[1 + (1 - q_{inter})B_{inter}|Q|]^{1/(1-q_{inter})}$. Top left: For the exchange rate of the U.S. Dollar against the British Pound, the index S&P500, the IBM stock and crude oil (West Texas Intermediate (WTI)), from left to right in the plot; the corresponding values for $q_{inter}$ are 0.95, 0.92, 0.97, 0.927 (with $A = 2$, 2.04, 1.95, 2.02 and $B_{inter} = 240$, 175, 95, 60). Similarly for the top right, bottom left and bottom right plots. From [107].

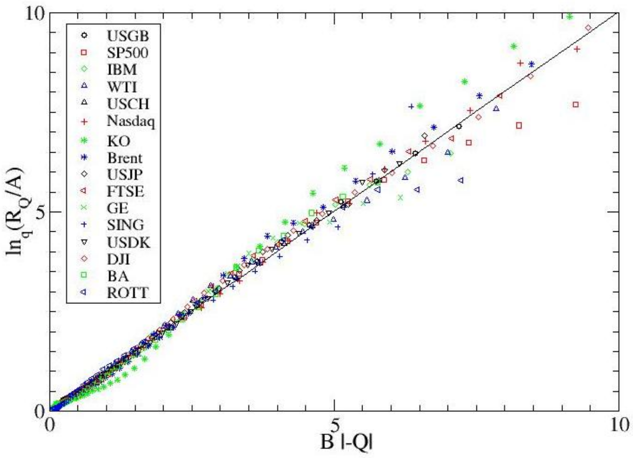


**Figure 8.** The mean inter-occurrence time $R_Q$ versus the absolute value of the loss threshold $-Q$: $\ln_{q_{inter}}(R_Q/A)$ versus the $B_{inter}|-Q|$ representation of the same data of Figure 7. The continuous curve is a fitting with $R_Q = Ae_{q_{inter}}^{B_{inter}|-Q|}$. From [107].

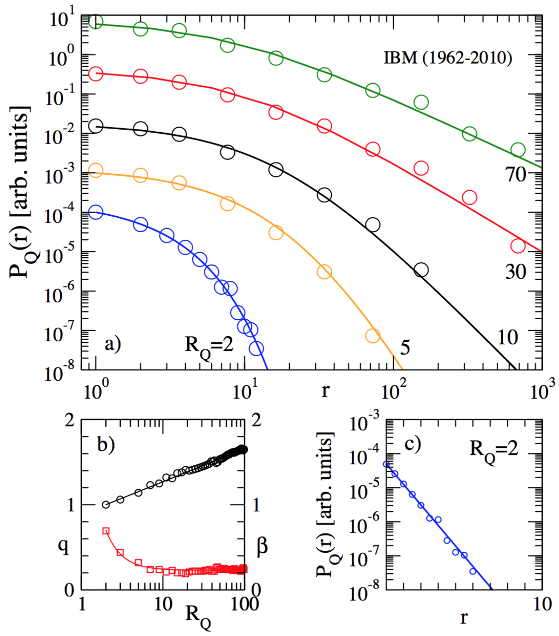


**Figure 9.** (**a**) The distribution function of the inter-occurrence times for the relative daily price returns $X_i$ of IBM in the period 1962–2010. The data points belong to $R_Q$ = 2, 5, 10, 30 and 70 (in units of days), from bottom to top. The full lines show the fitted $q$-exponentials $p_Q(r) \propto e_{q_{threshold}}^{-\beta_{threshold}\, r}$ for typical values of $R_Q$. (**b**) The dependence of the parameters $\beta_{threshold}$ (squares, lower curve) and $q_{threshold}$ (circles, upper curve) on $R_Q$ in the $q_{threshold}$-exponential. (**c**) Confirmation that, for $R_Q = 2$, the distribution function is a simple exponential (i.e., $q_{threshold} = 1$). The straight line is proportional to $2^{-r}$. From [106].

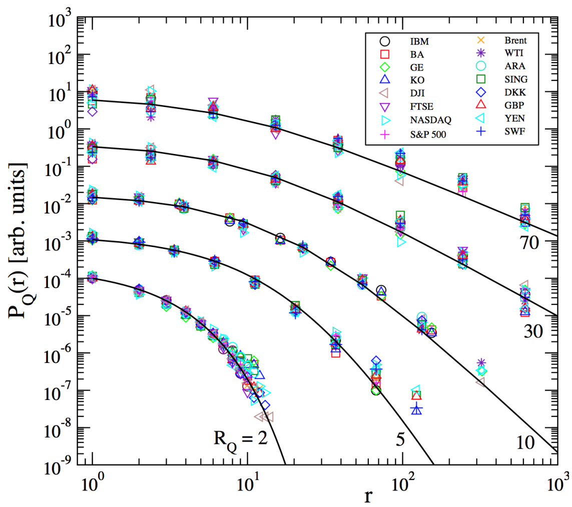


**Figure 10.** The distribution function of the inter-occurrence times (as in Figure 9a) for the relative daily price returns of 16 examples of financial data, taken from different asset classes (stocks, indices, currencies, commodities). The assets are: (i) the stocks of IBM, Boeing (BA), General Electric (GE), Coca-Cola (KO); (ii) the indices Dow Jones (DJI), Financial Times Stock Exchange 100 (FTSE), NASDAQ, S&P 500; (iii) the commodities Brent Crude Oil, West Texas Intermediate (WTI), Amsterdam-Rotterdam-Antwerp gasoline (ARA), Singapore gasoline (SING); and (iv) the exchange rates of the following currencies versus the U.S. Dollar: Danish Crone (DKK), British Pound (GBP), Yen, Swiss Francs (SWF). The full lines show the fitted $q$-exponentials, which are the same as in Figure 9a. From [106].

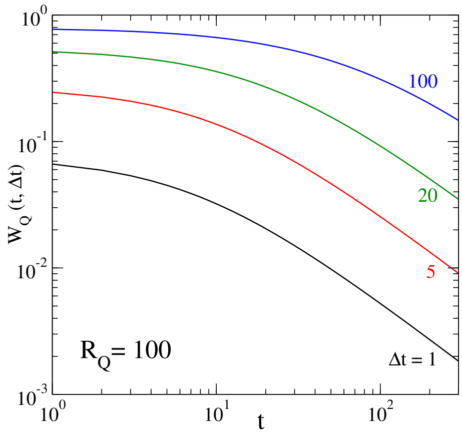


**Figure 11.** Universal risk function $W_Q(t, \Delta t)$ from Equation (23) for the inter-occurrence time $R_Q$ = 100 and for the intervals $\Delta t$ = 1, 5, 20, 100 days (from bottom to top). From [106].

## 2.4. Wealth

Wealth inequality within a given country is a classical and most important matter, which can be characterized within $q$-statistics as shown in [105]: see Figures 12 and 13. The larger the index $q_{inequality}$ is, the larger the inequality. As we verify, the U.K. and Germany are more egalitarian countries than the U.S. and Brazil. In addition to that, inequality appears to increase in the U.S. and Brazil, at least during the years indicated in the plots.

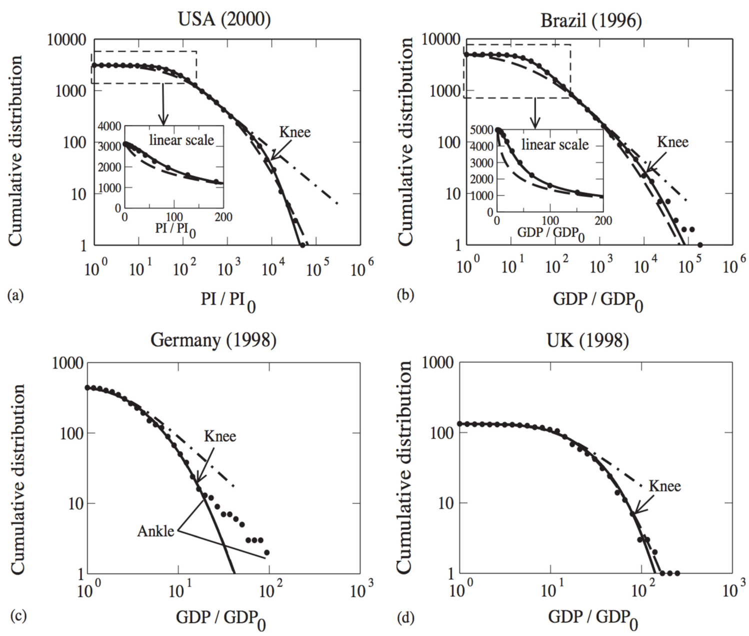


**Figure 12.** Binned inverse cumulative distribution of the county, $PI/PI_0$ (U.S.) and $GDP/GDP_0$ (Brazil, Germany and U.K.), where $PI$ denotes the Personal Income and $GDP$ denotes the Gross Domestic Product of countries. Three distributions are displayed for comparison: (i) $q$-Gaussian (with $\beta_{q'} = 0$) (dot-dashed); (ii) $(q; q')$-Gaussian (solid) and (iii) log-normal (dashed lines). (**a**,**b**) present insets with a linear-linear scale, to make more evident the quality of the fitting at the low region (in (**c**,**d**), the $(q; q')$-Gaussian and the log-normal curves are superposed and, so, are visually indistinguishable). The positions of the knees are indicated. The ankle is particularly pronounced in (c), though it is also present in the other cases. From [105], where further details are available.

Another index that characterizes the wealth of a country and its inequalities is associated with the prices of the land. See in Figure 14 (from [105]) an illustration for Japan, where $q_{land\ price} = 2.136$.

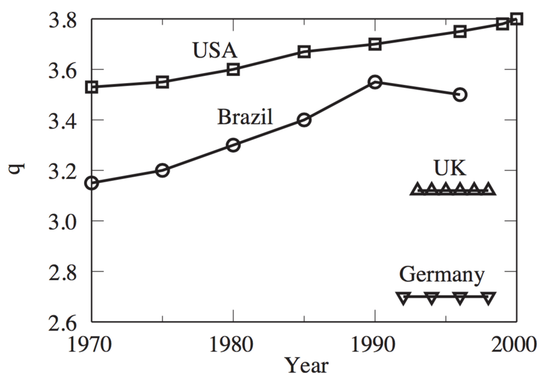


**Figure 13.** Evolution of parameter $q$ for the U.S. (squares), Brazil (circles), the U.K. (up triangles) and Germany (down triangles). The parameters $q'$ (for each country) are constant for all years: $q'_{Brazil} = 2.1$, $q'_{USA} = 1.7$, $q'_{Germany} = 1.5$, $q'_{UK} = 1.4$. Lines are only guides to the eyes. As we verify, in some cases, the index $q$ remains invariant along time, whereas in others, it evolves; the functional forms remain however the same as indicated in Figure 12. From [105].

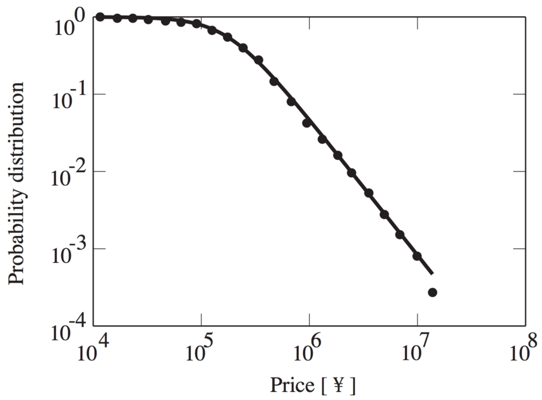


**Figure 14.** Inverse cumulative probability distribution of Japanese land prices for the year 1998. The solid curve is a $q$-Gaussian with $q = 2.136$, which corresponds to the slope $-1.76$, and $1/\sqrt{\beta_q} = 188{,}982$ Yen. From [105], where further details are available.

## 3. Conclusions and Perspectives

We have described a variety of financial and economic properties with a plethora of $q$-indices, such as $q_{return}$, $q_{volume}$, $q_{volatility}$, $q_{inter}$, $q_{threshold}$, $q_0$, $\tilde{q}$, $q_{inequality}$, $q_{land\ price}$. For a given system, how many independent indices should we expect? The full answer to this question remains up to now elusive. It seems however that only a few of them are essentially independent, all of the others being (possibly simple) functions of those few. Such an algebraic structure was first advanced and described in [119] and has been successfully verified in the solar wind [53] (see also [6] and the references therein) and elsewhere; it has recently been generalized [120,121] and related to the Moebius group. The central elements of these algebraic structures appear to constitute what is currently referred to in the literature as $q$-triplets [122]. The clarification and possible verification of such structures constitutes nowadays an important open question, whose further study would surely be most useful.

Another crucial question concerns the analytic calculation from first principles of some or all of the above $q$-indices. This is in principle possible (as illustrated in [63–66]), but it demands the complete knowledge of the microscopic model of the specific class of the complex system. For the full set of the $q$-indices shown in the present overview, such models are not available, even if they would be very welcome.

Let us finally emphasize that many other statistical approaches exist for the quantities focused on in the present overview. However, as announced in the title of this paper, this is out of the present scope. The present paper is one among various others belonging to the same Special Issue of the journal Entropy. The entire set of articles is expected to enable comparisons between these many approaches.

**Acknowledgments:** I thank C. Anteneodo, E.P. Borges, L. Borland, E.M.F. Curado, F.D. Nobre, R. Osorio, A.R. Plastino, S.M.D. Queiros, G. Ruiz, and U. Tirnakli for longstanding fruitful conversations. I thank especially J. Ludescher for authorizing me to use, in the present review, our unpublished figures of [107]. The financial support from CNPq and FAPERJ (Conselho Nacional de Desenvolvimento Cientifico e Tecnologico, and Fundacao de Amparo a Pesquisa do Rio de Janeiro, Brazilian funding agencies) and from the John Templeton Foundation (U.S.) are also gratefully acknowledged.

**Conflicts of Interest:** The author declares no conflict of interest.

## References

1. Penrose, O. *Foundations of Statistical Mechanics: A Deductive Treatment*; Pergamon: Oxford, UK, 1970; p. 167.
2. Tsallis, C. Possible generalization of Boltzmann–Gibbs statistics. *J. Stat. Phys.* **1988**, *53*, 479–487.
3. Curado, E.M.F.; Tsallis, C. Generalized statistical mechanics: Connection with thermodynamics. *J. Phys. A* **1991**, *24*, L69–L72.
4. Tsallis, C.; Mendes, R.S.; Plastino, A.R. The role of constraints within generalized nonextensive statistics. *Physica A* **1998**, *261*, 534–554.
5. Gell-Mann, M.; Tsallis, C. (Eds.) *Nonextensive Entropy-Interdisciplinary Applications*; Oxford University Press: New York, NY, USA, 2004.
6. Tsallis, C. *Introduction to Nonextensive Statistical Mechanics-Approaching a Complex World*; Springer: New York, NY, USA, 2009.
7. Muskat, M. *The Flow of Homogeneous Fluids through Porous Media*; McGraw-Hill: New York, NY, USA, 1937.
8. Frank, T.D. *Nonlinear Fokker–Planck Equations: Fundamentals and Applications*; Series Synergetics; Springer: Berlin, Germany, 2005.
9. Tsallis, C.; Bukman, D.J. Anomalous diffusion in the presence of external forces: Exact time-dependent solutions and their thermostatistical basis. *Phys. Rev. E* **1996**, *54*, R2197–R2200.
10. Combe, G.; Richefeu, V.; Stasiak, M.; Atman, A.P.F. Experimental validation of nonextensive scaling law in confined granular media. *Phys. Rev. Lett.* **2015**, *115*, 238301.
11. Plastino, A.R.; Plastino, A. Non-extensive statistical mechanics and generalized Fokker–Planck equation. *Physica A* **1995**, *222*, 347–354.
12. Nonextensive Statistical Mechanics and Thermodynamics. Available online: http://tsallis.cat.cbpf.br/biblio.htm (accessed on 29 August 2017).
13. Anteneodo, C.; Tsallis, C. Breakdown of exponential sensitivity to initial conditions: Role of the range of interactions. *Phys. Rev. Lett.* **1998**, *80*, 5313–5316.
14. Rapisarda, A.; Pluchino, A. Nonextensive thermodynamics and glassy behavior. *Europhys. News* **2005**, *36*, 202–206.
15. Chavanis, P.-H.; Campa, A. Inhomogeneous Tsallis distributions in the HMF model. *Eur. Phys. J. B* **2010**, *76*, 581–611.
16. Cirto, L.J.L.; Assis, V.R.V.; Tsallis, C. Influence of the interaction range on the thermostatistics of a classical many-body system. *Physica A* **2014**, *393*, 286–296.
17. Christodoulidi, H.; Tsallis, C.; Bountis, T. Fermi–Pasta–Ulam model with long-range interactions: Dynamics and thermostatistics. *EPL* **2014**, *108*, 40006.
18. Christodoulidi, H.; Bountis, T.; Tsallis, C.; Drossos, L. Dynamics and Statistics of the Fermi–Pasta–Ulam $\beta$–model with different ranges of particle interactions. *JSTAT* **2016**, 123206.
19. Bagchi, D.; Tsallis, C. Sensitivity to initial conditions of $d$-dimensional long-range-interacting quartic Fermi–Pasta–Ulam model: Universal scaling. *Phys. Rev. E* **2016**, *93*, 062213.

20. Bagchi, D.; Tsallis, C. Long-ranged Fermi–Pasta–Ulam systems in thermal contact: Crossover from $q$-statistics to Boltzmann–Gibbs statistics. *Phys. Lett. A* **2017**, *381*, 1123–1128.
21. Lucena, L.S.; da Silva, L.R.; Tsallis, C. Departure from Boltzmann–Gibbs statistics makes the hydrogen-atom specific heat a computable quantity. *Phys. Rev. E* **1995**, *51*, 6247–6249.
22. Nobre, F.D.; Tsallis, C. Infinite-range Ising ferromagnet-thermodynamic limit within generalized statistical mechanics. *Physica A* **1995**, *213*, 337–356.
23. Caride, A.O.; Tsallis, C.; Zanette, S.I. Criticality of the anisotropic quantum Heisenberg model on a self-dual hierarchical lattice. *Phys. Rev. Lett.* **1983**, *51*, 145–147.
24. Miritello, G.; Pluchino, A.; Rapisarda, A. Central limit behavior in the Kuramoto model at the 'edge of chaos'. *Physica A* **2009**, *388*, 4818–4826.
25. Tirnakli, U.; Tsallis, C.; Lyra, M.L. Circular-like maps: sensitivity to the initial conditions, multifractality and nonextensivity. *Eur. Phys. J. B* **1999**, *11*, 309–315.
26. Baldovin, F.; Robledo, A. Universal renormalization-group dynamics at the onset of chaos in logistic maps and nonextensive statistical mechanics. *Phys. Rev. E* **2002**, *66*, R045104.
27. Baldovin, F.; Robledo, A. Nonextensive Pesin identity. Exact renormalization group analytical results for the dynamics at the edge of chaos of the logistic map. *Phys. Rev. E* **2004**, *69*, R045202.
28. Mayoral, E.; Robledo, A. Tsallis' $q$ index and Mori's $q$ phase transitions at edge of chaos. *Phys. Rev. E* **2005**, *72*, 026209.
29. Tirnakli, U.; Tsallis, C.; Beck, C. A closer look at time averages of the logistic map at the edge of chaos. *Phys. Rev. E* **2009**, *79*, 056209.
30. Luque, B.; Lacasa, L.; Robledo, A. Feigenbaum graphs at the onset of chaos. *Phys. Lett. A* **2012**, *376*, 3625, doi:10.1016/j.physleta.2012.10.050.
31. Tirnakli, U.; Borges, E.P. The standard map: From Boltzmann–Gibbs statistics to Tsallis statistics. *Nat. Sci. Rep.* **2016**, *6*, 23644.
32. Douglas, P.; Bergamini, S.; Renzoni, F. Tunable Tsallis Distributions in Dissipative Optical Lattices. *Phys. Rev. Lett.* **2006**, *96*, 110601.
33. Bagci, G.B.; Tirnakli, U. Self-organization in dissipative optical lattices. *Chaos* **2009**, *19*, 033113.
34. Lutz, E.; Renzoni, F. Beyond Boltzmann–Gibbs statistical mechanics in optical lattices. *Nat. Phys.* **2013**, *9*, 615–619.
35. Liu, B.; Goree, J. Superdiffusion and non-Gaussian statistics in a driven-dissipative 2D dusty plasma. *Phys. Rev. Lett.* **2008**, *100*, 055003.
36. Bouzit, O.; Gougam, L.A.; Tribeche, M. Screening and sheath formation in a nonequilibrium mixed Cairns-Tsallis electron distribution. *Phys. Plasmas* **2015**, *22*, 052112.
37. DeVoe, R.G. Power-law distributions for a trapped ion interacting with a classical buffer gas. *Phys. Rev. Lett.* **2009**, *102*, 063001.
38. Pickup, R.M.; Cywinski, R.; Pappas, C.; Farago, B.; Fouquet, P. Generalized spin glass relaxation. *Phys. Rev. Lett.* **2009**, *102*, 097202.
39. Tsallis, C.; de Souza, A.M.C.; Maynard, R. Derivation of Lévy-type anomalous superdiffusion from generalized statistical mechanics. In *Lévy Flights and Related Topics in Physics*; Shlesinger, M.F., Zaslavsky, G.M., Frisch, U., Eds.; Springer: Berlin, Germany, 1995; p. 269.
40. Tsallis, C.; Levy, S.V.F.; de Souza, A.M.C.; Maynard, R. Statistical-mechanical foundation of the ubiquity of Levy distributions in nature. *Phys. Rev. Lett.* **1995**, *75*, 3589–3593.
41. CMS Collaboration. Transverse-momentum and pseudorapidity distributions of charged hadrons in pp collisions at $\sqrt{s} = 0.9$ and 2.36 TeV. *J. High Energy Phys.* **2010**, *2*, 41, doi:10.1007/JHEP02(2010)041.
42. CMS Collaboration. Transverse-momentum and pseudorapidity distributions of charged hadrons in *pp* collisions at $\sqrt{s} = 7$ TeV. *Phys. Rev. Lett.* **2010**, *105*, 022002.
43. Marques, L.; Andrade, E., II; Deppman, A. Nonextensivity of hadronic systems. *Phys. Rev. D* **2013**, *87*, 114022.
44. Marques, L.; Cleymans, J.; Deppman, A. Description of high-energy pp collisions using Tsallis thermodynamics: Transverse momentum and rapidity distributions. *Phys. Rev. D* **2015**, *91*, 054025.
45. Tsallis, C.; Arenas, Z.G. Nonextensive statistical mechanics and high energy physics. *EPJ* **2014**, *71*, 00132.
46. ALICE Collaboration. $K^*(892)^0$ and $\Phi(1020)$ meson production at high transverse momentum in pp and Pb-Pb collisions at $\sqrt{s_{NN}} = 2.76\,TeV$. *Phys. Rev. C* **2017**, *95*, 064606.

47. Oliveira, H.P.; Soares, I.D. Dynamics of black hole formation: Evidence for nonextensivity. *Phys. Rev. D* **2005**, *71*, 124034.
48. Komatsu, N.; Kimura, S. Entropic cosmology for a generalized black-hole entropy. *Phys. Rev. D* **2013**, *88*, 083534.
49. Silva, V.H.C.; Aquilanti, V.; de Oliveira, H.C.B.; Mundim, K.C. Uniform description of non-Arrhenius temperature dependence of reaction rates, and a heuristic criterion for quantum tunneling vs. classical non-extensive distribution. *Chem. Phys. Lett.* **2013**, *590*, 201–207.
50. Antonopoulos, C.G.; Michas, G.; Vallianatos, F.; Bountis, T. Evidence of $q$-exponential statistics in Greek seismicity. *Physica A* **2014**, *409*, 71–77.
51. Upadhyaya, A.; Rieu, J.-P.; Glazier, J.A.; Sawada, Y. Anomalous diffusion and non-Gaussian velocity distribution of *Hydra* cells in cellular aggregates. *Physica A* **2001**, *293*, 549–558.
52. Bogachev, M.I.; Kayumov, A.R.; Bunde, A. Universal internucleotide statistics in full genomes: A footprint of the DNA structure and packaging? *PLoS ONE* **2014**, *9*, e112534.
53. Burlaga, L.F.; Vinas, A.F. Triangle for the entropic index $q$ of non-extensive statistical mechanics observed by Voyager 1 in the distant heliosphere. *Physica A* **2005**, *356*, 375–384.
54. Burlaga, L.F.; Ness, N.F. Magnetic field strength fluctuations and the $q$-triplet in the heliosheath: Voyager 2 observations from 91.0 to 94.2 AU at latitude 30° S. *Astrophys. J.* **2013**, *765*, 35.
55. Moyano, L.G.; Tsallis, C.; Gell-Mann, M. Numerical indications of a $q$-generalised central limit theorem. *Europhys. Lett.* **2006**, *73*, 813–819.
56. Thistleton, W.J.; Marsh, J.A.; Nelson, K.P.; Tsallis, C. $q$-Gaussian approximants mimic non-extensive statistical-mechanical expectation for many-body probabilistic model with long-range correlations. *Cent. Eur. J. Phys.* **2009**, *7*, 387–394.
57. Chavanis, P.-H. Nonlinear mean field Fokker–Planck equations. Application to the chemotaxis of biological population. *Eur. Phys. J. B* **2008**, *62*, 179–208.
58. Umarov, S.; Tsallis, C.; Steinberg, S. On a $q$-central limit theorem consistent with nonextensive statistical mechanics. *J. Math.* **2008**, *76*, 307–328.
59. Umarov, S.; Tsallis, C.; Gell-Mann, M.; Steinberg, S. Generalization of symmetric $\alpha$-stable Lévy distributions for $q > 1$. *Math. Phys.* **2010**, *51*, 033502.
60. Nelson, K.P.; Umarov, S. Nonlinear statistical coupling. *Physica A* **2010**, *389*, 2157–2163.
61. Hanel, R.; Thurner, S.; Tsallis, C. Limit distributions of scale-invariant probabilistic models of correlated random variables with the $q$-Gaussian as an explicit example. *Eur. Phys. J. B* **2009**, *72*, 263–268.
62. Umarov, S.; Tsallis, C. The limit distribution in the $q$-CLT for $q \geq 1$ is unique and can not have a compact support. *J. Phys. A* **2016**, *49*, 415204.
63. Andrade, J.S., Jr.; da Silva, G.F.T.; Moreira, A.A.; Nobre, F.D.; Curado, E.M.F. Thermostatistics of overdamped motion of interacting particles. *Phys. Rev. Lett.* **2010**, *105*, 260601.
64. Vieira, C.M.; Carmona, H.A.; Andrade, J.S., Jr.; Moreira, A.A. General continuum approach for dissipative systems of repulsive particles. *Phys. Rev. E* **2016**, *93*, 060103(R).
65. Caruso, F.; Tsallis, C. Nonadditive entropy reconciles the area law in quantum systems with classical thermodynamics. *Phys. Rev. E* **2008**, 78, 021102.
66. Carrasco, J.A.; Finkel, F.; Gonzalez-Lopez, A.; Rodriguez, M.A.; Tempesta, P. Generalized isotropic Lipkin-Meshkov-Glick models: Ground state entanglement and quantum entropies. *J. Stat. Mech.* **2016**, *2016*, 033114.
67. Weinstein, Y.S.; Lloyd, S.; Tsallis, C. Border between between regular and chaotic quantum dynamics. *Phys. Rev. Lett.* **2002**, *89*, 214101.
68. Betzler, A.S.; Borges, E.P. Nonextensive distributions of asteroid rotation periods and diameters. *Astron. Astrophys.* **2012**, *539*, A158, doi:10.1051/0004-6361/201117767.
69. Betzler, A.S.; Borges, E.P. Nonextensive statistical analysis of meteor showers and lunar flashes. *Mon. Not. R. Astron. Soc.* **2015**, *447*, 765–771.
70. Li, Y.; Li, N.; Tirnakli, U.; Li, B.; Tsallis, C. Thermal conductance of the coupled-rotator chain: Influence of temperature and size. *EPL* **2017**, *117*, 60004.
71. Nivanen, L.; Le Mehaute, A.; Wang, Q.A. Generalized algebra within a nonextensive statistics. *Rep. Math. Phys.* **2003**, *54*, 437–444.

72. Borges, E.P. A possible deformed algebra and calculus inspired in nonextensive thermostatistics. *Physica A* **2004**, *340*, 95–101.
73. Tempesta, P. Group entropies, correlation laws, and zeta functions. *Phys. Rev. E* **2011**, *84*, 021121.
74. Ruiz, G.; Tsallis, C. Reply to comment on "towards a large deviation theory for strongly correlated systems". *Phys. Lett. A* **2013**, *377*, 491–495.
75. Jauregui, M.; Tsallis, C. New representations of $\pi$ and Dirac delta using the nonextensive- statistical-mechanics $q$-exponential function. *Math. Phys.* **2010**, *51*, 063304.
76. Sicuro, G.; Tsallis, C. $q$-Generalized representation of the d-dimensional Dirac delta and $q$-Fourier transform. *Phys. Lett. A* **2017**, *381*, 2583–2587.
77. Nobre, F.D.; Rego-Monteiro, M.A.; Tsallis, C. Nonlinear relativistic and quantum equations with a common type of solution. *Phys. Rev. Lett.* **2011**, *106*, 140601.
78. Costa Filho, R.N.; Almeida, M.P.; Farias, G.A.; Andrade, J.S., Jr. Displacement operator for quantum systems with position-dependent mass. *Phys. Rev. A* **2011**, *84*, 050102(R).
79. Mazharimousavi, S.H. Revisiting the displacement operator for quantum systems with position-dependent mass. *Phys. Rev. A* **2010**, *85*, 034102.
80. Nobre, F.D.; Rego-Monteiro, M.A.; Tsallis, C. A generalized nonlinear Schroedinger equation: Classical field-theoretic approach. *Europhys. Lett.* **2012**, *97*, 41001.
81. Rego-Monteiro, M.A.; Nobre, F.D. Nonlinear quantum equations: Classical field theory. *J. Math. Phys.* **2013**, *54*, 103302.
82. Rego-Monteiro, M.A.; Nobre, F.D. Classical field theory for a non-Hermitian Schroedinger equation with position-dependent masses. *Phys. Rev. A* **2013**, *88*, 032105.
83. Costa Filho, R.N.; Alencar, G.; Skagerstam, B.-S.; Andrade, J.S., Jr. Morse potential derived from first principles. *Europhys. Lett.* **2013**, *101*, 10009.
84. Toranzo, I.V.; Plastino, A.R.; Dehesa, J.S.; Plastino, A. Quasi-stationary states of the NRT nonlinear Schroedinger equation. *Physica A* **2013**, *392*, 3945–3951.
85. Curilef, S.; Plastino, A.R.; Plastino, A. Tsallis' maximum entropy ansatz leading to exact analytical time dependent wave packet solutions of a nonlinear Schroedinger equation. *Physica A* **2013**, *392*, 2631–2642.
86. Plastino, A.R.; Tsallis, C. Nonlinear Schroedinger equation in the presence of uniform acceleration. *J. Math. Phys.* **2013**, *54*, 041505.
87. Plastino, A.R.; Souza, A.M.C.; Nobre, F.D.; Tsallis, C. Stationary and uniformly accelerated states in nonlinear quantum mechanics. *Phys. Rev. A* **2014**, *90*, 062134.
88. Pennini, F.; Plastino, A.R.; Plastino, A. Pilot wave approach to the NRT nonlinear Schroedinger equation. *Physica A* **2014**, *403*, 195–205.
89. Da Costa, B.G.; Borges, E.P. Generalized space and linear momentum operators in quantum mechanics. *J. Math. Phys.* **2014**, *55*, 062105.
90. Nobre, F.D.; Rego-Monteiro, M.A. Non-Hermitian PT symmetric Hamiltonian with position-dependent masses: Associated Schroedinger equation and finite-norm solutions. *Braz. J. Phys.* **2015**, *45*, 79–88.
91. Plastino, A.; Rocca, M.C. From the hypergeometric differential equation to a non-linear Schroedinger one. *Phys. Lett. A* **2015**, *379*, 2690–2693.
92. Alves, L.G.A.; Ribeiro, H.V.; Santos, M.A.F.; Mendes, R.S.; Lenzi, E.K. Solutions for a q-generalized Schroedinger equation of entangled interacting particles. *Physica A* **2015**, *429*, 35–44.
93. Plastino, A.R.; Tsallis, C. Dissipative effects in nonlinear Klein–Gordon dynamics. *EPL* **2016**, *113*, 50005.
94. Plastino, A.; Rocca, M.C. Hypergeometric connotations of quantum equations. *Physica A* **2016**, *450*, 435–443.
95. Bountis, T.; Nobre, F.D. Travelling-wave and separated variable solutions of a nonlinear Schroedinger equation. *J. Math. Phys.* **2016**, *57*, 082106.
96. Nobre, F.D.; Plastino, A.R. A family of nonlinear Schroedinger equations admitting $q$-plane wave. *Phys. Lett. A* **2017**, *381*, 2457–2462.
97. Capurro, A.; Diambra, L.; Lorenzo, D.; Macadar, O.; Martin, M.T.; Mostaccio, C.; Plastino, A.; Rofman, E.; Torres, M.E.; Velluti, J. Tsallis entropy and cortical dynamics: The analysis of EEG signals. *Physica A* **1998**, *257*, 149–155.
98. Mohanalin, J.; Beenamol; Kalra, P.K.; Kumar, N. A novel automatic microcalcification detection technique using Tsallis entropy and a type II fuzzy index. *Comput. Math. Appl.* **2010**, *60*, 2426–2432.

99. Soares, D.J.B.; Tsallis, C.; Mariz, A.M.; Silva, L.R. Preferential attachment growth model and nonextensive statistical mechanics. *EPL* **2005**, *70*, 70–76.
100. Thurner, S.; Tsallis, C. Nonextensive aspects of self-organized scale-free gas-like networks. *Europhys. Lett.* **2005**, *72*, 197–203.
101. Brito, S.G.A.; da Silva, L.R.; Tsallis, C. Role of dimensionality in complex networks. *Nat. Sci. Rep.* **2016**, *6*, 27992.
102. Borland, L. Closed form option pricing formulas based on a non-Gaussian stock price model with statistical feedback. *Phys. Rev. Lett.* **2002**, *89*, 098701.
103. Tsallis, C.; Anteneodo, C.; Borland, L.; Osorio, R. Nonextensive statistical mechanics and economics. *Physica A* **2003**, 324, 89–100.
104. Osorio, R.; Borland, L.; Tsallis, C. Distributions of high-frequency stock-market observables. In *Nonextensive Entropy-Interdisciplinary Applications*; Gell-Mann, M., Tsallis, C., Eds.; Oxford University Press: New York, NY, USA, 2004.
105. Borges, E.P. Empirical nonextensive laws for the county distribution of total personal income and gross domestic product. *Physica A* **2004**, 334, 255–266.
106. Ludescher, J.; Tsallis, C.; Bunde, A. Universal behaviour of inter-occurrence times between losses in financial markets: An analytical description. *Europhys. Lett.* **2011**, *95*, 68002.
107. Ludescher, J. (Institut fur Theoretische Physik, Justus-Liebig-Universitat, Giessen, Germany); Tsallis, C. (Centro Brasileiro de Pesquisas Físicas and National Institute of Science and Technology for Complex Systems, Rio de Janeiro, Brazil). Private Communications, 2011.
108. Queiros, S.M.D. On generalisations of the log-Normal distribution by means of a new product definition in the Kapteyn process. *Physica A* **2012**, *391*, 3594–3606.
109. Bogachev, M.I.; Eichner, J.F.; Bunde, A. Effect of nonlinear correlations on the statistics of return intervals in multifractal data sets. *Phys. Rev. Lett.* **2007**, *99*, 240601.
110. Ludescher, J.; Bunde, A. Universal behavior of the inter-occurrence times between losses in financial markets: Independence of the time resolution. *Phys. Rev.* **2014**, *90*, 062809.
111. Perello, J.; Gutierrez-Roig, M.; Masoliver, J. Scaling properties and universality of first-passage-time probabilities in financial markets. *Phys. Rev. E* **2011**, *84*, 066110.
112. Ruseckas, J.; Kaulakys, B.; Gontis, V. Herding model and $1/f$ noise. *EPL* **2011**, *96*, 60007.
113. Ruseckas, J.; Gontis, V.; Kaulakys, B. Nonextensive statistical mechanics distributions and dynamics of financial observables from the nonlinear stochastic differential equations. *Adv. Complex Syst.* **2012**, *15*, 1250073.
114. Gontis, V.; Kononovicius, A. A consentaneous agent based and stochastic model of the financial markets. *PLoS ONE* **2014**, *9*, e102201.
115. Biondo, A.E.; Pluchino, A.; Rapisarda, A. Modeling financial markets by self-organized criticality. *Phys. Rev. E* **2015**, *92*, 042814.
116. Biondo, A.E.; Pluchino, A.; Rapisarda, A. Order book, financial markets, and self-organized criticality. *Chaos Solitons Fractals* **2016**, *88*, 196–208.
117. Biondo, A.E.; Pluchino, A.; Rapisarda, A. A multilayer approach for price dynamics in financial markets. *Eur. Phys. J. Spec. Top.* **2017**, *226*, 477–488.
118. Ruiz, G.; Fernandez, A. Evidence for criticality in financial data. *arXiv* **2017**, arXiv:1702.06191.
119. Tsallis, C.; Gell-Mann, M.; Sato, Y. Asymptotically scale-invariant occupancy of phase space makes the entropy $S_q$ extensive. *Proc. Natl. Acad. Sci. USA* **2005**, *102*, 15377–15382.
120. Tsallis, C. Generalization of the possible algebraic basis of $q$-triplets. *Eur. Phys. J. Spec. Top.* **2017**, *226*, 455–466.
121. Tsallis, C. Statistical mechanics for complex systems: On the structure of q-triplets. In Proceedings of the 31st International Colloquium on Group Theoretical Methods in Physics, Rio de Janeiro, Brazil, 20–24 July 2016.
122. Tsallis, C. Dynamical scenario for nonextensive statistical mechanics. *Physica A* **2004**, *340*, 1–10, doi:10.1016/j.physa.2004.03.072.